

Application-Driven Learning via Joint Prediction and Optimization of Demand and Reserves Requirement

Joaquim Dias Garcia

LAMPS, DEE, PUC-Rio & PSR-Inc, Rio de Janeiro, Brazil, joaquim@psr-inc.com

Alexandre Street

LAMPS, DEE, PUC-Rio, Rio de Janeiro, Brazil, street@ele.puc-rio.br

Tito Homem-de-Mello

School of Business, UAI, Santiago, Chile, tito.hmello@uai.cl

Francisco D. Muñoz

Facultad de Ingeniería y Ciencias, UAI, Santiago, Chile, fdmunoz@uai.cl

Forecasting and decision-making are generally modeled as two sequential steps with no feedback, following an open-loop approach. In power systems, operators first forecast loads trying to minimize errors with respect to historical data. They also size reserve requirements based on error estimates. Next, energy and reserves are scheduled and the system is operated following the dispatch schedule, deploying reserves as needed to accommodate forecast errors. However, co-optimizing these processes may lead to better decisions and result in lower operating costs than when they are considered sequentially. In this paper, we present a new closed-loop learning framework in which the processes of forecasting and decision-making are merged and co-optimized through a bilevel optimization problem. We prove asymptotic convergence of the method and propose two solution approaches: an exact method based on the KKT conditions of the second level problem, and a scalable heuristic approach suitable for decomposition methods. We benchmark our methodology with the standard sequential least squares forecast and dispatch planning process. We apply the proposed methodology to an illustrative single-bus system and to the IEEE 24-, 118-, and 300-bus test systems. Our results show that the proposed approach yields consistently better performance than the standard open-loop approach.

Key words: Application-driven learning, joint prediction and optimization, bilevel optimization, reserves scheduling, forecast, power systems planning

1. Introduction

The most common approach to make decisions under uncertainty involves three steps. In the first step, one develops a forecast for all uncertainties that affect the decision-making problem based on all information available. In the second step, an action based on the forecast is selected. Finally, in the third step, one implements corrective actions after uncertainties are realized. This three-step procedure constitutes an open-loop forecast-decision process in which the outcomes of the decisions are not considered in the forecasting framework.

In the electricity sector, it is common for system operators to use an open-loop forecast-decision approach. First, loads are forecast based on standard statistical techniques, such as least squares (LS), and reserve requirements are defined by simple rules, based on quantiles, extreme values and standard deviation of forecast errors according to specified reliability standards (Ela et al. 2011). Then, a decision is made to allocate generation resources following an energy and reserve scheduling program (Chen et al. 2013, De Vos et al. 2019). In real-time, reserves are deployed to ensure that power is balanced at every node, compensating for forecast errors.

From the academic perspective, it has been demonstrated that stochastic programming models yield better results than deterministic ones when making decisions under uncertainty because the former takes distributions into consideration. These models provide better results in terms of cost, reliability, and market efficiency compared to deterministic approaches (Wang and Hobbs 2014). Nevertheless, in practical applications, two issues arise: proper modeling of distributions is challenging and tractability imposes small sample sizes for techniques like sample average approximations (SAA). A consequence of this tractability issue is that SAA solutions become sample dependent (Papavasiliou et al. 2014, Papavasiliou and Oren 2013), thereby compromising market transparency and preventing stakeholders acceptance (Wang and Hobbs 2015). Therefore, most system operators worldwide still rely on deterministic short-term scheduling (economic dispatch or unit commitment) models with exogenous forecasts for loads and reserve requirements (Chen et al. 2013, PJM 2018). Within this context, one alternative to improve the performance of deterministic

scheduling tools is to forecast load and reserve requirements with the goal of minimizing energy and reserve scheduling costs.

There is empirical evidence that system operators rely on *ad hoc* or out-of-market actions—and not just on reserves—to deal with uncertainty in operations. According to the 2019 Annual Report on Market Issues and Performance of the California ISO (CAISO 2020), “...operators regularly take significant out-of-market actions to address the net load uncertainty over a longer multi-hour time horizon (e.g., 2 or 3 hours). These actions include routine upward biasing of the hour-ahead and 15-minute load forecast, and exceptional dispatches to commit and begin to ramp up additional gas-fired units in advance of the evening ramping hours.” Additionally, reserve requirements are, in practice, empirically defined according to further *ad hoc* off-line rules based on off-line analysis (Ela et al. 2011, PJM 2018). These *ad hoc* procedures lack technical formalism and transparency to minimize operating and reliability costs. Consequently, this challenging real-world application requires further research observing the practical issues that need to be addressed to improve the current state-of-the-art of industry practices.

For years, decision-making and forecasting have been treated as two completely separate processes (Bertsimas and Kallus 2019). Many communities, such as Statistics and Operations Research, have studied these problems and developed multiple tools combining probability and optimization. The machine learning community, which combines many ideas from optimization and probability, has also been tackling such tasks and has proposed methods to treat them jointly (Bengio 1997).

Classical forecasting methods do not take the underlying application of the forecast into account. Consequently, hypotheses such as prediction error symmetry in least squares (LS) might not be the best fit for problems with asymmetric outcomes. By acknowledging the asymmetry in particular problems, researchers have attempted to capture it empirically; however, such an approach does not take the application into account directly. Some existing methods do capture asymmetry, such as Quantile Regression (QR) (Rockafellar et al. 2008). The interest in exploring asymmetric loss functions is not new. For instance, Zellner (1986a) and Zellner (1986b) acknowledge that

biased estimators can perform even better than those that make accurate predictions of statistical properties of the stochastic variables. The author exemplifies that an overestimation is not as bad as underestimation for the case of dam construction and attributes a second example about the asymmetry on real estate assessment to Varian (1975).

Within this context, two possible avenues of research are opened to achieve better results: i) a focus on improving the decision-making model (prescriptive framework), which assumes we can change it to consider embedded co-optimized forecasts (Bertsimas and Kallus 2019); or ii) a focus on improving the forecasting model (predictive framework), which assumes we can not change the decision-making process (in our application, defined by system operators' dispatch models), but we can change the forecasts to incorporate, in a closed-loop manner, a given application cost function (Bengio 1997, Elmachtoub and Grigas 2017, Muñoz et al. 2020). Therefore, in this paper, we focus on the latter avenue. In Section 2, we provide a literature review on this subject.

1.1. Objective and contribution

The objective of this paper is to present a new closed-loop application-driven learning framework for point forecast of elements of an optimization model. In this new framework, both *ex-ante* (planning) and *ex-post* (implementation) cost-minimization structures of the decision-maker, i.e., the *application schema*, are considered in the prediction process. Therefore, our framework replaces the traditional statistical error minimization objective with a cost-minimization structure of a specific application. To do that, we derive a new and flexible learning framework based on a bilevel optimization model. Furthermore, we provide an asymptotic convergence proof for both the objective function value and estimated parameters. This paper focuses on applying the general method to the demand and reserve requirement forecasting problem of power system operators.

The first-level of our bilevel problem seeks the parameters of a forecasting model that performs best in terms of the application objective, i.e., *ex-ante* reserves allocation cost plus *ex-post*, or real-time, energy dispatch costs incurred when operating the system under the observed demand data. Thus, the first-level accounts for both the predictive model specification (parameters selection)

and the cost evaluation metric based on the actual operation of the system for many data points. It is relevant to mention that we can also consider reserve requirement constraints imposed by regulatory rules, reliability standards (The European Commission 2017, Ela et al. 2011), and risk-aversion metrics (Shapiro et al. 2014). In the second level, the *ex-ante* energy and reserve scheduling process of the system operator is accounted for based on 1) the conditional demand forecast, and 2) the reserve requirements, both defined in the first level for each point of the historical data considered in the training set. Thus, in our bilevel model, we have multiple parallel lower-level problems, each of which representing the one-step-ahead deterministic two-stage scheduling process performed by the system operator for each point of the training dataset. In this context, the second level ensures closed-loop feedback characterizing joint scheduling decisions of energy and reserve allocations without perfect information of the target period data.

Two solutions approaches are presented. The first approach is an exact method based on the KKT conditions of the second-level problem. The second is a scalable heuristic approach suitable for decomposition methods and parallel computing. Although not limited to linear bilevel programs, we show how to design efficient methods tailored for off-the-shelf linear optimization solvers. Additionally, our scalable heuristic method ensures optimal second-level solutions. This is a salient feature of our method. In this context, the proposed framework is general and suitable for a wide range of applications relying on the standard structure of the forecast-decision process.

We benchmark our methodology with the traditional sequential least squares forecast and energy and reserve scheduling approach. We apply the proposed methodology to multiple case studies, namely, an illustrative single-bus system and the IEEE 24-, 118-, and 300-bus test systems. Results show that the proposed approach yields consistently better performance in out-of-sample tests than the benchmark where forecasts and decisions are sequentially carried out. More specifically, by comparing the newly proposed exact and heuristic methods, we show that the heuristic approach is capable of consistently achieving high-quality solutions. For larger systems, where the exact method fails to find solutions within reasonable computational times, the heuristic method still exhibits high-quality performance compared to the benchmark for all test systems.

2. Literature Review

We review literature on 1) forecast models jointly optimized for a given application, hereinafter referred to as application-driven forecast, and 2) uncertainty forecasting and reserve sizing.

2.1. Application-driven forecast models

The ingenious idea of integrating the process of forecasting and optimizing a downstream problem was first proposed in the seminal paper by Bengio (1997). More than twenty years ago, the author emphasized the importance of estimating parameters with the correct goals in mind. In that work, a Neural Network (NN) is trained to forecast stocks with an objective function that describes the portfolio revenue given an allocation based on stocks forecast. An attempt to lower the burden of the method was proposed by Garcia and Gençay (2000); the idea is to train multiple prediction models with standard regressions, but choose the best one in the out-of-sample analysis considering the proper application-driven objective function. The work by Kao et al. (2009) presents another intermediary methodology. The model for estimating forecasts includes both the application objective function and the fitness measure similar to maximum likelihood estimation (MLE). A bi-objective problem is solved with scalarization; the authors look for a good balance between MLE and application value.

Following the key idea of Bengio (1997) closely, the work by Donti et al. (2017) presents a generic algorithm to deal with parameter optimization of forecasting models embedded in stochastic programming problems, that is, parameters estimated considering the loss function of the actual problem. The algorithm is based on the stochastic gradient descent (SGD) method and employs tools for automatically differentiating strongly convex quadratic optimization problems. The method is applied to small prototypical quadratic programming problems and the local solutions obtained are shown to be promising.

More recently, the work Smart “Predict and Optimize” (SPO) (Elmachtoub and Grigas 2017), recognizes the importance of the closed-loop estimation. The authors develop an algorithm for the

linear programming case that is based on relaxation and convexification of the nonlinear loss function before applying a tailored SGD approach, instead of looking for local solutions with nonlinear methods. To develop the algorithm, the authors limit themselves to linear dependency on features and restrict uncertainty to the objective function. SPO is similar to the method proposed by Ryzhov and Powell (2012) to estimate uncertain objective coefficients without considering features in a different context.

While working on this paper for a few months, the authors became aware of a recently posted preprint that guards many conceptual similarities to the general version of our proposed model. The work of Muñoz et al. (2020) also focuses on the idea of finding the best forecast for a given application (or context) through a bilevel framework. The framework proposed in Muñoz et al. (2020) is applied to estimate a parameter of the inverse demand curve of a Cournot strategic producer bidding in forward markets. The scalability of their model relies on a nonlinear relaxation of the right-hand-side of the complementarity constraints. In our method, we adopt a different approach to overcome the issue of suboptimal lower-level solutions and to tackle very large scale problems, as will explained in Section 7.4. Moreover, we prove convergence of our method, whereas Muñoz et al. (2020) do not discuss this theme.

Sen and Deng (2018) describes the so-called Learning Enabled Optimization (LEO). LEO is a framework to combine Statistical Learning (SL), Machine Learning (ML) and (stochastic) Optimization. The idea is to compare a set of predefined SL/ML models with the cost value of the actual application in mind. The main difference here is that the ML/SL are still estimated based on classical methods.

Not surprisingly, some of the above works either explicitly or implicitly formulate the problems as bilevel optimization problems. For more information on bilevel optimization the reader is directed to Bard (2013). The work by Dempe (2018) lists hundreds of references related to bilevel optimization, including papers related to parameter optimization. Parameter optimization is frequently modeled as bilevel optimization and has been drawing the attention of many fields such as ML,

control, energy systems, and game theory. This can be thought of as a version of the closed-loop paradigm since these works target the best parameters for algorithms and applications. We refer to (Franceschi et al. 2018) for applications in hyper-parameter tuning. Under a broader ML umbrella, our methodology can be seen as a ML forecast approach where the *application schema* is embedded into the method through its explicit mathematical programming formulation.

2.2. Uncertainty forecasting and reserve sizing

The operation of power systems has been profoundly related to uncertainty handling. The electric load has been among the main challenges for forecasters in power systems for many years. Researchers around the world have proposed the most varied methodologies, ranging from standard linear regressions to Neural Networks (NN); these techniques, along with many others, are reviewed in Hong and Fan (2016) and Van der Meer et al. (2018). Variable renewable energy sources are probably the current big challenge in forecasting for power systems. Although many techniques are already available, forecasting sources like wind have proven to be significantly harder than load (Van der Meer et al. 2018, Orwig et al. 2014). As shown in reviews (Sweeney et al. 2020, Van der Meer et al. 2018), wind and solar forecasting are divided into two main trends: i) physical-based methods that rely on topographic models and Numerical Weather Predictions; ii) statistical methods including Kalman filters, ARMA models, and NN.

Although forecast methods have consistently improved in the last years, the systems must be ready to withstand deviations from predicted values. The widely used approach is to allocate reserves in addition to the power scheduled to each generator to meet demand forecasts. The additional power is scheduled as reserve margins to give the system operator flexibility to handle real-time operation. Many methods have been proposed to account for the variations in loads, contingencies, and VRE (Holtinen et al. 2012). Furthermore, different reserve sizing rules are applied by different ISOs all over the world (Ela et al. 2011). These rules vary from deterministic *ad hoc* procedures to more statistical-oriented guidelines.

In Ela et al. (2011), examples of real-life *ad hoc* procedures to allocate reserves are presented, most of them relying on static approaches. Although time-varying reserves have been studied in the past, they have re-emerged as dynamic probabilistic reserve (De Vos et al. 2019). In the context of a more sophisticated dynamic probabilistic reserve approach, probabilistic forecasts are frequently used to account for the forecasting errors. These probabilistic reserves can be sized following a variety of method with different complexity based on: forecast error standard deviations (Strbac et al. 2007, Holttinen et al. 2012), non-parametric estimation of the forecast error distribution (Bucksteeg et al. 2016), or even machine learning (De Vos et al. 2019). These are all considered stochastic methods and are simple alternatives to capture and incorporate fairly complex dynamics that are challenging for bottom-up approaches (De Vos et al. 2019).

A prominent alternative to the use of reserves in power systems is the Stochastic Unit commitment. In such application, many types of reserves can be defined endogenously targeting cheaper operations on average. However, as described in the review on Unit Commitment by Zheng et al. (2014), there are at least three main barriers toward the wide acceptance of stochastic unit commitment: i) uncertainty modeling, ii) computational performance, and iii) market design. Uncertainty modeling is jointly tackled by statistical modeling of the uncertainty concerning scenario generation and forecasting and by a decision-making framework like risk-averse stochastic optimization, robust optimization, and so on. Computational performance is the focus of many works like the Lagrangian decomposition (Aravena and Papavasiliou 2020), improved formulations (Knueven et al. 2020), progressive hedging (Gade et al. 2016). Notwithstanding the relevant recent advances in this area, the computational burden and the consequential instability of solutions under small sample sizes still preclude the acceptance of stochastic UC models by ISOs. Finally, the least studied challenge is the market design. It requires experimenting and developing rules that are both feasible to be implemented and accepted by stakeholders (Kazempour et al. 2018, Wang and Hobbs 2015). Based on previously reported industry practices and since ISOs currently follow the alternate route and tackle the uncertainty of UC with reserves (Wang and Hobbs 2015), we will also follow this approach to propose a readily practical method.

3. Application-Driven Learning and Forecasting

In this section, we contrast the standard sequential framework, referred to as *open-loop*, and the joint prediction and optimization model, referred to as *closed-loop*. The presentation is in general form to facilitate the description of the solution algorithm, to set notation for the convergence results and to highlight that the method has applications beyond load forecasting and reserve sizing in power systems. We will specialize the bilevel optimization problem for closed-loop load forecasting and reserve sizing in Section 6.

We consider a dataset of historical data $\{y_t, x_t\}_{t \in \mathbb{T}}$, where $\mathbb{T} = \{1, \dots, T\}$. Here y_t are observations of a variable of interest that we want to forecast, while x_t are observations of external variables (covariates or features) that can be used to explain the former. Furthermore, the latter might include lags of y_t as in auto-regressive time series models. Additionally, it is worth mentioning that both y_t and x_t can be vector valued.

The classic forecast-decision approach works as follows. The practitioner *trains* a parametric *forecast* model seeking for the best vector of parameters, θ , such that a loss function, $l(\cdot, \cdot)$, between the conditional forecast for sample t , $\hat{y}_t(\theta, x_t)$, and the actual data, y_t , is minimized, i.e., solving $\min_{\theta} \frac{1}{T} \sum_t l(\hat{y}_t(\theta, x_t), y_t)$. This is frequently done by solving LS optimization problems and finding $\theta^{LS} \in \arg \min_{\theta} \frac{1}{T} \sum_t \|\hat{y}_t(\theta, x_t) - y_t\|^2$. In the *planning* step, a decision is made by an optimized policy based on the previously obtained forecast, i.e., with $\hat{y}_t^{LS} = \hat{y}_t(\theta^{LS}, x_t)$. This results in a vector $z^*(\hat{y}_t^{LS})$, which in our application comprises the schedule of energy and reserves through generating units. Finally, the actual data y_t is observed, and the decision-maker must adapt to it, for instance, the system operator responds with a balancing re-dispatch, and a *cost*, $G_a(z^*(\hat{y}_t^{LS}), y_t)$, is measured. There is no feedback of the final cost into the forecasting and decision policy, hence, the name *open-loop*.

3.1. The proposed closed-loop application-driven framework

The core of the proposed predictive framework is to explore a feedback structure between the estimated predictive model and the application cost assessment. The general idea is depicted in Figure 1 that stresses the difference from the open-loop model.

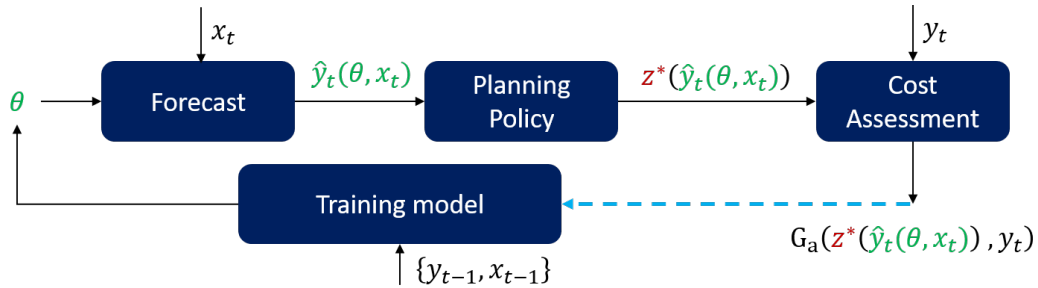


Figure 1 Learning models: considering the blue dashed line we have the *closed-loop* model, otherwise it represents the *open-loop* model.

The estimation method can be mathematically described through the following bilevel optimization problem (BOP):

$$\theta_T = \arg \min_{\theta \in \Theta, \hat{y}_t, z_t^*} \frac{1}{T} \sum_{t \in \mathbb{T}} G_a(z_t^*, y_t) \quad (1)$$

$$s.t. \quad \hat{y}_t = \Psi(\theta, x_t) \quad \forall t \in \mathbb{T} \quad (2)$$

$$z_t^* \in \arg \min_{z \in Z} G_p(z, \hat{y}_t) \quad \forall t \in \mathbb{T}, \quad (3)$$

where, for $i \in \{a, p\}$,

$$G_i(z, y) = c_i^\top z + Q_i(z, y) \quad (4)$$

$$Q_i(z, y) = \min_u \{q_i^\top u \mid W_i u \geq b_i - H_i z + F_i y\} \quad (5)$$

Note that the functions in (4) and (5) resemble the formulation of two-stage stochastic programs, in the sense that given a decision z and an observation y , one determines the best corrective action u . In that context, c_i , q_i , W_i , b_i , H_i and F_i ($i \in \{a, p\}$) are parameters defined according to the problem of interest. Note also that the uncertainty y appears only on the right-hand side of the problems defining Q_a and Q_p ; this will be important for our convergence analysis and solutions methods.

In model (1)–(5), $\Psi(\theta, x_t)$ represents a forecasting model that depends on both the vector of parameters, θ , and the features vector, x_t , possibly including lags of y_t . The vector \hat{y}_t is the forecast generated for sample (or period) t (comprising load and reserve requirements) conditioned to the

vector of features, x_t , as defined in (2). For each t , the forecast \hat{y}_t is used as input in a second-level problem and a decision planning policy, z_t^* , is obtained as a function of \hat{y}_t , i.e., $z_t^*(\hat{y}_t)$. This is done by optimizing the decision-maker *planning* cost function, $G_p(z, \hat{y}_t)$ in (3). Then, the optimized policy z_t^* is evaluated in the first level against the actual realization, y_t , for each t . The evaluation is made under the decision-maker's *assessment* (or *evaluation*) cost function, $G_a(z_t^*(\hat{y}_t), y_t)$. Hence, the application is embedded into the estimation process in both the *ex-ante* planning policy and *ex-post* evaluation objective (1)–(5). It is worth noticing that the proposed formulation can be interpreted as an optimization over θ in a back-test, in which for a given θ , the assessment of the forecast performance is completely determined by $G_a(z_t^*(\hat{y}_t), y_t)$. Within this context, the upper level identifies the parameters with the best back-test performance. Furthermore, note that for a fixed θ , there is no coupling between two samples, thereby the model can be decomposed per t . This will be used in one of the proposed solution methods. Finally, there is a slight abuse of notation in (1) because the argmin only retrieves θ_T , the solution for θ with T samples, thus disregarding the rest of the first level decision vectors, \hat{y}_t and z_t^* .

One key difference from previous works (Donti et al. 2017, Elmachtoub and Grigas 2017, Muñoz et al. 2020) is that G_a and G_p can be different functions. This is extremely useful in the context of power systems operations where planning models might differ from real-time ones. Although model (1)–(5) is fairly general, we specialize to the case of linear programs and right-hand-side uncertainty, (4)–(5), because we will assume polyhedral structure for the set Z . This can be contrasted with previous works that considered strongly quadratic programs (Donti et al. 2017) and objective uncertainty (Elmachtoub and Grigas 2017). As mentioned earlier, this specialization will be important for developing our asymptotic convergence results and our solution methods.

4. Convergence Results

In this section, we discuss some conditions for convergence of estimators obtained with application-driven joint prediction and optimization. Again, our goal is to obtain the best possible forecast \hat{y}_t , but this is completely defined by the parameters θ since x_t is known. Let θ_T be the optimal

solution of (1)–(5) considering T data points. We will show that θ_T converges to one element of the solution set of the actual expected value formulation of the problem (as opposed to the previously presented sampled version). We will start describing some assumptions, then we will state and prove the main theorem.

Assumption 1 *The solution set of the optimization problem in (3) is a singleton for all possible values of \hat{y}_t .*

In other words, the problem is always feasible and the solution is always unique. This is not as restrictive as it seems. The feasibility requirement is similar to the classical assumption of complete recourse in stochastic programming. The uniqueness requirement is equivalent to the absence of dual degeneracy in a linear program (Borrelli et al. 2003). In the case the problem in question is dual-degenerate, it is possible to eliminate this degeneracy by perturbing the objective function—in our case, the vectors c_p and q_p —with small numbers that do not depend on the right-hand-side (RHS) of the problem. Thus, the same perturbation is valid for all possible \hat{y}_t (Megiddo and Chandrasekaran 1989). Another possibility would be resorting to some lexicographic simplex method (Nocedal and Wright 2006). In this setting, we can define the set-valued function:

$$\zeta(y) := \operatorname{argmin}_{z \in Z} G_p(z, y) \quad (6)$$

From Böhm (1975) we know that if $\zeta(y)$ is a compact set for all y then it is a continuous set-valued function. Moreover, since $\zeta(y)$ is a singleton for all possible values of y , then we treat it as a vector-valued function which is continuous and piece-wise affine (Borrelli et al. 2003).

Assumption 2 *The feasibility set Z that appears in (3) is a non-empty and bounded polyhedron.*

Assumption 2 is reasonable since this is the set of implementable solutions of the decision-maker, typically representing physical quantities.

Assumption 3 *The feasibility set of the dual of the problem that defines $Q_a(z, y)$ in (5) is non-empty and bounded.*

Note that this set does not depend on z and y , since they appear in the RHS of the primal problem. Again, this assumption is akin to a relatively complete recourse assumption applied to the problem defining the outer-level function.

We state now our main convergence result.

THEOREM 1. Consider the process given by (1)–(5) and its output θ_T . Suppose that (i) Assumptions 1, 2 and 3 hold, (ii) the forecasting function $\Psi(\cdot, \cdot)$ is continuous in both arguments, (iii) the data process $(X_1, Y_1), \dots, (X_T, Y_T)$ is independent and identically distributed (with (X, Y) denoting a generic element), (iv) the random variable Y is integrable, and (v) the set Θ is compact. Then,

$$\lim_{T \rightarrow \infty} d(\theta_T, S^*) = 0, \quad (7)$$

where d is the Euclidean distance from a point to a set and S^* is defined as

$$S^* = \operatorname{argmin}_{\theta \in \Theta} \mathbb{E} [G_a(\zeta(\Psi(\theta, X)), Y)], \quad (8)$$

with $\zeta(\cdot)$ defined in (6).

Proof: First, notice that $G_i(z, Y)$, $i \in \{a, p\}$, is continuous with respect to its arguments as it is a sum of a linear function and the optimal value of a parametric program (Gal 2010). Recall that ζ is a continuous vector-valued function because of Assumption 1. Hence, $G_a(\zeta(\Psi(\theta, X)), Y)$ is a real-valued continuous function. In the sequel, we show that $G_a(\zeta(\Psi(\theta, X)), Y)$ is integrable. Indeed, since Z is bounded (Assumption 2), it follows that $\zeta(y)$ is bounded for all x by a constant, say K_1 , so that $\|\zeta(y)\| \leq K_1$. By duality, $Q_i(z, y) = \max_{\pi} \{(b_i - H_i z + F_i y)^\top \pi \mid W_i^\top \pi = q_i, \pi \geq 0\}$, but by Assumption 3 the dual variables of $Q_a(z, y)$ are bounded by a constant, say K_2 , so $\|\pi\| \leq K_2$. Thus, by a sequence of applications of Cauchy-Schwarz and triangle inequalities, we have that

$$\begin{aligned} |G_a(\zeta(\Psi(\theta, X)), Y)| &\leq |c_a^\top \zeta(\Psi(\theta, X)) + Q_a(\zeta(\Psi(\theta, X)), Y)| \\ &\leq \|c_a\| \|\zeta(\Psi(\theta, X))\| + \|b_a - H_a \zeta(\Psi(\theta, X)) + F_a Y\| \max_{W_i^\top \pi = q_a, \pi \geq 0} \|\pi\| \\ &\leq K_1 \|c_a\| + K_2 (\|b_a\| + \|H_a \zeta(\Psi(\theta, X))\| + \|F_a Y\|) \\ &\leq K_1 \|c_a\| + K_2 (\|b_a\| + \|H_a\| K_1 + \|F_a\| \|Y\|). \end{aligned}$$

Hence, since Y is integrable (condition (iv) of the Theorem), we have that $G_a(\zeta(\Psi(\theta, X)), Y)$ is integrable.

It follows that the conditions of Theorem 7.53 in Shapiro et al. (2014) are satisfied and we conclude that: (i) the function $\varphi(\theta) := \mathbb{E}[G_a(\zeta(\Psi(\theta, X)), Y)]$ is finite valued and continuous in θ , (ii) by the Strong Law of Large Numbers, for any $\theta \in \Theta$ we have

$$\lim_{T \rightarrow \infty} \frac{1}{T} \sum_{t=1}^T G_a(\zeta(\Psi(\theta, X_t)), Y_t) = \mathbb{E} [G_a(\zeta(\Psi(\theta, X)), Y)] \quad \text{w.p.1}, \quad (9)$$

and (iii) the convergence in (9) is *uniform* in θ . Thus, by Theorem 5.3 in Shapiro et al. (2014), since the set Θ is compact we have that the minimizers (over Θ) of the expression on the left-hand side of (9)—i.e., θ_T —converge to the minimizers of the expression on the right-hand side in the sense of (7)–(8). *Q.E.D.*

Remark 1 *Assumption 3 can be replaced by assuming a compact support of Y ; in this case, $G_a(z, y)$ is a continuous function, where both arguments are defined on compact sets, hence it attains a maximum and is trivially integrable.*

Remark 2 *Condition (iii) of Theorem 1 clearly precludes modeling the situation where the features x_t include (functions of) previous observations y_{t-1}, \dots, y_{t-k} . However, since the i.i.d. assumption is used only to allow for the application of the Strong Law of Large Numbers in (9), in the case where the x_t include lagged observations of $\{y_t\}$, one may be able to replace (9) with a more general convergence result for stochastic processes—for instance, the fundamental result on convergence of long-run averages for ergodic Markov chains.*

5. Solution Methodology

In this section, we describe solution methods to estimate the forecasting model within the proposed application-driven closed-loop framework described in (1)–(5). First, we present an exact method based on an equivalent single-level mixed integer linear programming (MILP) reformulation of the bilevel optimization problem (1)–(5). This method uses MILP-based linearization techniques to

address the Karush Kuhn Tucker (KKT) optimality conditions of the second level and thereby guarantee global optimality of the solution in exchange for limited scalability. In the sequence, we describe how to use zero-order methods (Conn et al. 2009) that do not require gradients to develop an efficient and scalable heuristic method to achieve high-quality solutions to larger instances. These methods will leverage existing optimization solvers, their current implementations and features.

5.1. MILP-based exact method

Our first approach consists of solving the bilevel problem (1)–(3) with standard techniques based on the KKT conditions of the second-level problem (Fortuny-Amat and McCarl 1981). Thus, the resulting single-level nonlinear equivalent formulation can be reformulated as a MILP and solved by standard commercial solvers. The conversion between KKT form to MIP form can be done by numerous techniques (Siddiqui and Gabriel 2013, Pereira et al. 2005, Fortuny-Amat and McCarl 1981), all of which have pros and cons. These techniques are implemented and automatically selected by the open-source package BilevelJuMP.jl (Dias Garcia et al. 2021). This new package was conceived to allow users to formulate bilevel problems in JuMP (Dunning et al. 2017) and solve them with multiple off-the-shelf optimization solvers.

For the sake of completeness we write the single-level nonlinear reformulation of the bilevel problem (1)–(5) in (10)–(14). For simplicity, in this model we assume that $Z = \{z | Ax \geq h\}$ and that Θ is polyhedral.

$$\min_{\theta \in \Theta, \hat{y}_t, z_t^*, u_t, \pi_t} \frac{1}{T} \sum_{t \in \mathbb{T}} [c_a^\top z_t^* + Q_a(z_t^*, y_t)] \quad (10)$$

$$s.t. \quad \forall t \in \mathbb{T}:$$

$$\hat{y}_t = \Psi(\theta, x_t) \quad (11)$$

$$W_p y_t + H_p z_t^* \geq b_p + F_p \hat{y}_t; \quad A z_t^* \geq h \quad (12)$$

$$W_p^\top \pi_t = q_p; \quad H_p^\top \pi_t + A^\top \mu_t = c_p; \quad \pi_t, \mu_t \geq 0 \quad (13)$$

$$\pi_t \perp W_p u_t + H_p z_t^* - b_p - F_p \hat{y}_t; \quad \mu_t \perp A z_t^* - h \quad (14)$$

Equations (10) and (11) are the same as (1) and (2). (3) was replaced by (12)–(14). (12) are the primal feasibility constraint, (13) are the dual feasibility constraints, and (14) represents the complementarity constraints.

5.2. Scalable heuristic method

The proposed class of methods will make extensive use of the way of thinking described in the Figure 1. In other words, the core algorithm decomposes the problem as follows: We call this

Algorithm 1: Meta algorithm

Result: Optimized θ

Initialize θ ;

while *Not converged* **do**

 Update θ ;

for $t \in \mathbb{T}$ **do**

 Forecast: $\hat{y}_t \leftarrow \Psi(\theta, x_t)$;

 Plan Policy: $z_t^* \leftarrow \arg \min_{z \in Z} G_p(z, \hat{y}_t)$;

 Cost Assessment: $cost_t \leftarrow G_a(z_t^*, y_t)$

end

 Compute cost: $cost(\theta) \leftarrow \sum_{t \in \mathbb{T}} (cost_t)$

end

method a meta-algorithm because a few steps are not well specified, namely *Initialization*, *Update*, and *Convergence* check, allowing for a wide range of possible specifications. *Initialization* can be as simple as θ receiving a vector of zeros, which might not be good if the actual algorithm is a local search. One alternative that will be applied in the case study section is the usage of traditional models as starting points, for instance, the ordinary least squares. In the case study, we will initialize the algorithm with the LS estimate, this guarantees that the algorithm will return at most the same cost as the open-loop framework in the training sample. There are many possibilities for

the *convergence* test. For instance, iteration limit, time, the variation of the objective function value, and other algorithm-specific tests. Finally, the *update* step depends on the selected concrete algorithm that is ultimately minimizing the non-trivial $cost(\theta)$ function.

We will focus on a derivative-free local search algorithm named Nelder-Mead (Conn et al. 2009). Notwithstanding, it is relevant to highlight the generality of the proposed meta-algorithm. For instance, gradient-based algorithms could also be developed based on numerical differentiation and automatic differentiation (Nocedal and Wright 2006). In this context, gradient calculation would enable the usage of Gradient Descent and BFGS-like algorithms (Nocedal and Wright 2006).

The main features of the above-proposed meta-algorithm are: 1) it is suitable for parallel computing (the loop in the sample \mathbb{T} is intrinsically decoupled); 2) each step is based on a deterministic LP defining the second-level variables in (3), suitable for off-the-shelf commercial solvers that find globally optimal solutions in polynomial time; 3) each inner step can significantly benefit from warm-start processes developed in linear programming solvers (e.g., the dual simplex warm-start is extremely powerful, and many times only a handful of iterations will be needed in comparison to possibly thousands of iteration needed if there were no warm-start, cf. Nocedal and Wright (2006)). It is worth emphasizing that the aforementioned feature 2) allows for an exact (always optimal) description of the second-level problem. In our approach, we keep the second level exact and face the challenge of optimizing a nonlinear problem on the upper level. In contrast, Muñoz et al. (2020) choose to relax the complementarity constraints and deal with a nonlinear program not benefited by the above mentioned features 1) to 3). As will be illustrated in our case study, this choice is supported by empirical evidence about the shape of the nonlinear function faced in the objective function. Additionally, it is usual in more complex estimation processes (like maximum likelihood-based methods) to rely on nonlinear optimization methods to select the best parameters (Henningsen and Toomet 2011). Moreover, although not convex, as explored in our case study, the objective function exhibits relevant properties that facilitate the search within the parameters domain.

One caveat is that variations on θ can lead to possibly infeasible results for the *Policy Planning* and *Cost Assessment* optimization problems. Consequently, we require complete recourse for such problems. In cases where this property does not hold, it is always possible to add artificial (slack) variables with high penalty costs in the objective function to keep the problem feasible. In the energy and reserve dispatch problem, this requirement is addressed by imbalance variables (load and renewable curtailment decisions).

6. Application-Driven Load Forecasting and Reserve Sizing

In this work, we focus on the energy and reserve scheduling problem of power systems (Chen et al. 2013, Kirschen and Strbac 2018). In this problem, we aim to obtain the best joint conditional point-forecast for the vector of nodal demands, \hat{D}_t , and vectors of up and down zonal or nodal reserve requirements, $\hat{R}_t^{(up)}$ and $\hat{R}_t^{(dn)}$. While the forecast vector of nodal loads represent, e.g., the next hour operating point target that system operators and agents should comply with, up- and down-reserve requirements represent a forecast of system's resource availability (or security margins), defined per zone or node, allowing the system to withstand load deviations. Note that we can think of loads as a general net load that corresponds to load minus non-dispatchable (e.g., renewable) generation.

The inputs of the problem are: vectors of historical data of dependent and explanatory variables, $\{y_t, x_t\}_{t \in \mathbb{T}}$, including lags of demand, D_{t-1}, \dots, D_{t-k} , and possibly other covariates such as climate and dummy variables; vectors of data associated with generating units; maximum generation capacity, G , dispatch costs or offers, c ; maximum up- and down-reserve capacity, $\bar{r}^{(up)}$ and $\bar{r}^{(dn)}$; up- and down-reserves costs, $p^{(up)}$ and $p^{(dn)}$; load shedding and spillage penalty costs, λ^{LS} and λ^{SP} ; network data comprising the vector of transmission line capacities F ; and network sensitivity matrix, B , describing the network topology and physical laws of electric circuits. Additionally, it is important to mention that the input data describing the system characteristics can be provided under two perspectives: 1) under the perspective of the actual *ex-post* (or assessed/implemented) operation, i.e., based on the observed demand data and most accurate system's description for

evaluating the function G_a defined in (1); and 2) under the *ex-ante* planning perspective, G_p , which is accounted for in (3) based on observed features, such as previous information, and system operator's description of the system considered in the dispatch tool. While the former has already been listed at the beginning of this paragraph, the latter uses the same symbols but with a tilde above, i.e., $\tilde{c}, \tilde{p}^{(up)}, \tilde{p}^{(dn)}, \tilde{G}, \tilde{B}$, etc. For a simple matrix representation of the problem, we define e to be a vector with one in all entries and appropriate dimension. M is an incidence matrix with buses in rows and generators in columns that is one when the generator lies in that bus and zero otherwise. Similarly, N is an incidence matrix with generators in columns and reserve zones in rows, which is one if the generator lies in that area. Thus, we study the following particularization of the closed-loop framework proposed in (1)–(5):

$$\min_{\substack{\theta_D, \theta_{R^{up}}, \theta_{R^{dn}}, \\ \hat{D}_t, \hat{R}_t, g_t, \delta_t^{LS}, \delta_t^{SP}, \\ g_t^*, r_t^{(up)*}, r_t^{(dn)*}}} \frac{1}{T} \sum_{t \in \mathbb{T}} [c^\top g_t + p^{(up)\top} \hat{r}_t^{(up)*} + p^{(dn)\top} \hat{r}_t^{(dn)*} + \lambda^{LS} \delta_t^{LS} + \lambda^{SP} \delta_t^{SP}] \quad (15)$$

s.t. $\forall t \in \mathbb{T}$:

$$\hat{D}_t = \Psi_D(\theta_D, x_t) \quad (16)$$

$$\hat{R}_t^{(up)} = \Psi_{R^{(up)}}(\theta_{R^{(up)}}, x_t) \quad (17)$$

$$\hat{R}_t^{(dn)} = \Psi_{R^{(dn)}}(\theta_{R^{(dn)}}, x_t) \quad (18)$$

$$e^T (M g_t - \delta_t^{SP}) = e^T (D_t - \delta_t^{LS}) \quad (19)$$

$$-F \leq B(M g_t + \delta_t^{LS} - D_t - \delta_t^{SP}) \leq F \quad (20)$$

$$g_t^* - r_t^{(dn)*} \leq g_t \leq g_t^* + r_t^{(up)*} \quad (21)$$

$$\delta_t^{LS}, \delta_t^{SP}, \hat{R}_t^{(up)}, \hat{R}_t^{(dn)}, g_t \geq 0 \quad (22)$$

$$\left(g_t^*, r_t^{(up)*}, r_t^{(dn)*} \right) \in \arg \min_{\substack{\hat{g}_t, \hat{\delta}_t^{LS}, \hat{\delta}_t^{SP}, \\ \hat{r}_t^{(up)}, \hat{r}_t^{(dn)}}} [\tilde{c}^\top \hat{g}_t + \tilde{p}^{(up)\top} \hat{r}_t^{(up)} + \tilde{p}^{(dn)\top} \hat{r}_t^{(dn)} + \tilde{\lambda}^{LS} \hat{\delta}_t^{LS} + \tilde{\lambda}^{SP} \hat{\delta}_t^{SP}] \quad (23)$$

$$s.t. \quad e^T (M \hat{g}_t - \hat{\delta}_t^{SP}) = e^T (\hat{D}_t - \hat{\delta}_t^{LS}) \quad (24)$$

$$-\tilde{F} \leq \tilde{B}(M \hat{g}_t + \hat{\delta}_t^{LS} - \hat{D}_t - \hat{\delta}_t^{SP}) \leq \tilde{F} \quad (25)$$

$$N \hat{r}_t^{(up)} = \hat{R}_t^{(up)} \quad (26)$$

$$N\hat{r}_t^{(dn)} = \hat{R}_t^{(dn)} \quad (27)$$

$$\hat{g}_t + \hat{r}_t^{(up)} \leq \tilde{G} \quad (28)$$

$$\hat{g}_t - \hat{r}_t^{(dn)} \geq 0 \quad (29)$$

$$\hat{r}_t^{(up)} \leq \bar{r}^{(up)} \quad (30)$$

$$\hat{r}_t^{(dn)} \leq \bar{r}^{(dn)} \quad (31)$$

$$\hat{g}_t, \hat{r}_t^{(up)}, \hat{r}_t^{(dn)}, \hat{\delta}_t^{LS}, \hat{\delta}_t^{SP} \geq 0. \quad (32)$$

In (15)–(32), the objective function of the upper level problem (15) comprises the sum of the actual operating cost, the cost of scheduled reserves, and the implemented load shed and renewable spillage costs for all periods within the dataset, i.e., for $t \in \mathbb{T}$. In the upper level, constraints (16)–(18) define the forecast model. Note that all periods are coupled by the vector of parameters $\theta = [\theta_D^\top, \theta_{R^{(up)}}^\top, \theta_{R^{(dn)}}^\top]^\top$, which do not depend on t . These parameters define the forecast model that will be applied to each t for demand, as per \hat{D}_t in (16), for up reserve requirements, as per $\hat{R}_t^{(up)}$ in (17), and for down reserve requirements, as per $\hat{R}_t^{(dn)}$ in (18). The forecast models are defined by functions Ψ_D , $\Psi_{R^{(up)}}$, and $\Psi_{R^{(dn)}}$ that transform parameters and the historical data on load and reserve requirement forecasts. For the sake of simplicity and didactic purposes, in this work, we assume affine regression models. The reserves are parts of the forecast vector \hat{y}_t because the method optimizes a model for them. However, reserves historical data need not be in y_t , since, typically, the choice of reserves in each period is not based on past values of reserves.

Constraints (19)–(22) together with the objective function (15) particularize G_a from (1). They assess the *ex-post* operating cost (first term, $c_t^T g_t$, and the last to terms, $\lambda_t^{LS} \delta_t^{LS} + \lambda_t^{SP} \delta_t^{SP}$) of the actual dispatch given the *ex-ante* planned generation, g_t^* , and allocated up and down reserves, $r_t^{(up)*}$ and $r_t^{(dn)*}$, defined by the second level (23)–(32). Constraint (19) accounts for the *ex-post* energy balance constraint, where total generation meets total observed load data. The left-hand-side of the constraint is the sum of generated energy in all buses, with Mg_t resulting on the nodal generation injection vector (total generation per bus). δ_t^{SP} represents the nodal generation spilled

per bus (positive load imbalance decision). The right-hand-side of the constraint accounts for the net-nodal load vector (observed net-demand vector D_t). δ_t^{LS} represents the decision vector of nodal load shed (negative load imbalance decision). Finally, constraint (20) limits the flow of energy through each transmission line to pre-defined bounds and (21) limits the *ex-post* generation to respect the operation range defined by the *ex-ante* planned generation, g_t^* , and allocated up and down reserves, $r_t^{(up)*}, r_t^{(dn)*}$. Constraint (22) ensures positiveness of slack, generation, and reserve requirement variables.

The planning policy defines variables g_t^* , $r_t^{(up)*}$, and $r_t^{(dn)*}$ under the conditional information available in vector x_t . These variables should respect the optimality of the market's or system operator's *ex-ante* scheduling (or planning policy), as per (23), based on the vector of load forecasts, \hat{D}_t , and vectors of reserve requirements, $\hat{R}_t^{(up)}$ and $\hat{R}_t^{(dn)}$, for the next period (e.g., hour). Again, it is relevant to note that this planning policy may differ from the actual *ex-post* implemented policy (based on the observed load data D_t) resulting on the actual operating cost considered in the objective function of the first level (15). Within this context, constraints (23)–(32) detail the second-level problem, which represents the optimization that takes place in the planning phase at each period to define a generation and reserve schedule for the next period. Thus, these constraints are particularizing the general model, G_p in (3). In the proposed closed-loop framework, (23) is key. It allows us to define, within a problem that seeks the best forecast model aiming to minimize the *ex-post* operation cost, the objective of an *ex-ante* scheduling problem minimizing energy and reserve costs for a conditioned load forecast (\hat{D}_t) and reserve requirements ($\hat{R}_t^{(up)}$ and $\hat{R}_t^{(dn)}$). Constraints (24) and (25) are similar to (19) and (20). Expressions (26) and (27) ensure that the total reserve requirements ($\hat{R}_t^{(up)}$ and $\hat{R}_t^{(dn)}$, which are considered as parameters for the lower-level problem) must be allocated among generators in the form of up and down reserves ($\hat{r}_t^{(up)}$ and $\hat{r}_t^{(dn)}$ – second-level decision vectors). Constraints (28) and (29) limit the scheduled generation and reserves range (up and down) to generators physical generation limits. Constraints (30) and (31) limit the maximum amount of reserves that can be allocated in each generating unit, and (32) ensures positiveness of the generation and reserve decision vectors of the second level.

The proposed application-driven framework provides system operators with the flexibility to either jointly optimize the load forecast and the reserve requirements or only one of them. Additionally, this model is powerful because the load forecasts and both the size and location of reserve requirements are defined in the best way possible to maximize the ex-post performance of the operation. While the lower level, (23)–(32), ensures an *ex-ante* generation schedule and reserve allocation compatible with the system operator’s information level (best schedule given the previous hour conditional forecast for t), the upper level selects the parameters of the forecast model aiming to minimize the average *ex-post* operating cost for a large dataset. In this sense, depending on the network details considered in the assessment part of the model, it also helps in mitigating reserve deliverability issues associated with *ad hoc* procedures used in industry practices.

In the next section, we will compare a few variants of this problem by optimizing all or some of the parameters θ_D , $\theta_{R^{(up)}}$, and $\theta_{R^{(dn)}}$.

7. Case Studies

This section presents case studies to demonstrate the methodology’s applicability and how the closed-loop framework can outperform the classic open-loop scheme in multiple variants of the load forecasting and reserve sizing problem defined in Section 6. First, we show that the Heuristic method of Section 5.2 can achieve close to optimal solutions in a fraction of the time required by the Exact method of Section 5.1. Second, we study the estimated parameters’ and forecasts’ empirical properties and contrast them with the classical least squares (LS) estimators. After that, we briefly explore how the method can estimate dynamic reserves. Moreover, we apply the method to highlight the relations between load-shed cost and the estimated parameters. Finally, we show that the heuristic algorithm finds good quality local-optimal parameters systematically outperforming the LS open-loop benchmark for instances far larger than those solved in previously reported works tackling closed-loop bilevel frameworks. We used the same Dell Notebook (Intel i7 8th Gen with 8 logical cores, 16Gb RAM) for all studies.

7.1. Power systems cases and datasets

We consider four power system cases throughout this section. The first is a single bus system defined by us, with 1 zone, 1 load (with long term average of 6) and 4 generators (with capacities 5, 5, 2.5, 2.5 and costs 1, 2, 4, 8). The other three are typical test systems, based on realistic networks, used by the power system community, namely, "IEEE 24bus rts" (38 lines, 33 generators, 17 loads, 4 zones), "IEEE 118 bus" (186 lines, 54 generators, 99 loads, 7 zones) and "IEEE 300 bus" (411 lines, 69 generators, 191 loads, 10 zones). The base datasets were obtained from PG-LIB-OPF (Babaeinejadsarookolae et al. 2019). The zone definition is standard for the 24 buses case. For the 118 and 300 bus cases, we used the zones defined by Li et al. (2015).

Henceforth, we will refer to the test systems by their number of buses. We only considered as loads the buses with positive demand in the original files. We performed some modifications in the case data: all flow limits were set to 75% their rate; we modified the demand values of the cases 24, 118 and 300 by the factors: 0.9, 1.3 and 0.9, respectively. These modifications were made to stress the systems. Deficit and generation curtailment costs were defined, respectively, as 8 and 3 times the most expensive generator cost. All generators were allowed to have up to 30% their capacity allocated to reserves, and their reserve allocation costs were set to 30% their nominal costs. We only considered the linear component of the generators' costs in all instances. In all datasets, we used demand values as the long-term average of AR(1) processes for each bus. The AR(1) coefficients were set to 0.9 and the AR(0) coefficients were set so that we get the desired long-term averages. For the sake of simplicity, load profiles were generated independently. The coefficient of variation of all simulated load stochastic processes was 0.4. Negative demands were truncated to zero, although they could represent an excess renewable generation.

7.2. Studied models and notation

In most of the following sections we will consider simple forecast models so that we can detail experiment results clearly. Therefore, unless otherwise mentioned, the model used to forecast loads in each node is the following:

$$\hat{D}_t = \Psi_D(\theta_D, x_t) = \theta_D(0) + \theta_D(1)D_{t-1}, \quad (33)$$

For the single bus case, we set the “real”, or population, values as $\theta_D(0) = 0.6$ and $\theta_D(1) = 0.9$, resulting in the long-term average $\theta_D(0)/(1 - \theta_D(1)) = 6$, defined in section 7.1. Because the stochastic model for loads is homoscedastic, we set the reserve models to $AR(0)$ – i.e., a number that does not depend on previous values of reserves – since it is customary to set the reserves just in terms of variability of loads:

$$\hat{R}_t^{(up)} = \Psi_{R^{(up)}}(\theta_{R^{(up)}}, x_t) = \theta_{R^{(up)}}(0), \quad (34)$$

$$\hat{R}_t^{(dn)} = \Psi_{R^{(dn)}}(\theta_{R^{(dn)}}, x_t) = \theta_{R^{(dn)}}(0). \quad (35)$$

7.3. Exact vs heuristic method comparison

In this first experiment, we aim to compare the exact and the heuristic methods to check the quality of the latter for an instance that the exact method is capable of reaching global optimal solutions. To that end, we consider the single bus test system.

We started by solving 10 instances for each $T \in \{15, 25, 50, 75\}$. All instances solved with the exact method converged within a gap lower than 0.1% using the Gurobi solver or stopped after two hours. The heuristic method was terminated when the objective function presented a decrease lower than 10^{-7} between consecutive iterations. We used a Nelder-Mead implementation found in Mogensen and Riseth (2018). To compare the results, we plotted the ratio of objective values in Figure 2 (a) and the time ratio in Figure 2 (b). We can observe that the heuristic method achieves high-quality solutions for almost all instances. Although the exact method is competitive for $T \in \{15, 25\}$, the heuristic method is much faster with average solve time of 4.4s, for $T = 50$, and 5.9s, for $T = 75$, compared to 1200s and 6670s for the the exact method. Four instances with $T = 75$ did not converge with the exact method after two hours.

Next, we further analyze the shape of the objective cost, G_a in (1), as a function of the parameters, θ , to better understand how good the heuristic solutions can be. Given one dataset with 250 points, we fixed the demand autoregressive parameters to the LS estimation and plot in \mathbb{R}^3 the cost as a function of the reserve requirement parameters. Two views of this function are presented in Figure

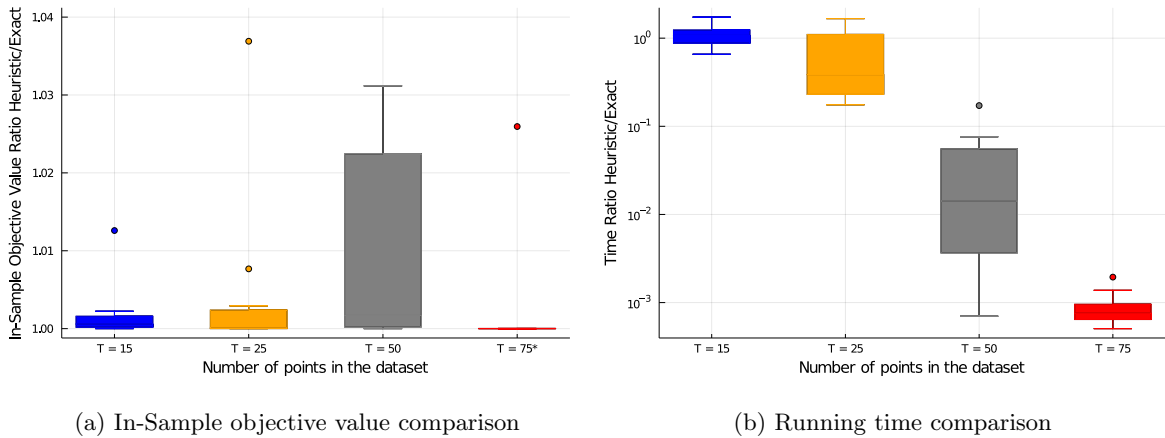


Figure 2 (a) Objective of Heuristic method divided by the objective of Exact method for the same datasets.

*Four problems not considered for $T = 75$: the exact method found no solution in the given time. (b) Time to solve the same problem (in log scale): Heuristic method divided by Exact method.

3 (a) and (b). We also plot the cost as a function of the $AR(0)$ and $AR(1)$ coefficients of the demand forecasting model, in this case, the reserve requirement parameters were fixed to the exogenous values of ± 1.96 standard deviations of the LS estimation of load forecast. This is presented in two views in Figure 3 (c) and (d).

We can note that both functions are reasonably well behaved, due to (3) possibly not convex, however, with a good shape for local search algorithms. This is a relevant feature supporting the choice for our heuristic approach as previously described at the end of Section 5.2. We also note a smoothing effect due to the average in the objective function (Shapiro et al. 2014). Therefore, it is expected to have more well-behaved functions as the sample size grows.

7.4. Asymptotic behavior and biased estimation

Now we focus only on the heuristic method to analyze how the estimates behave with respect to the dataset size variation. We will see that they actually converge in our experiments. Moreover, we empirically show through out-of-sample studies that using the closed-loop model is strictly better than the open-loop one provided we have a reasonable dataset size in the training step. It will be possible to see that a method with too many parameters might overfit the model for reduced

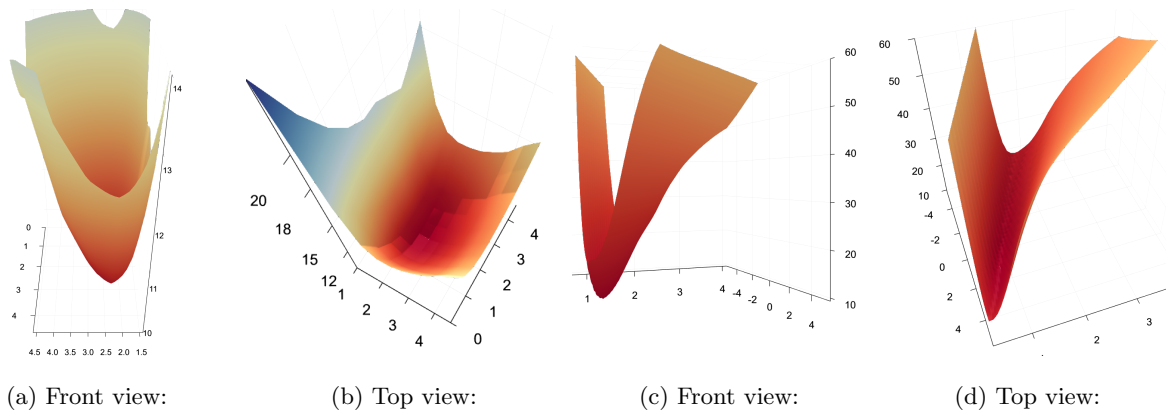


Figure 3 Training cost as a functions of optimization parameters. (a) and (b): fixed load AR coefficients, optimizing reserves $\theta_{R^{(up)}}(0), \theta_{R^{(dn)}}(0)$. (c) and (d): fixed reserves, optimizing load AR coefficients $\theta_D(0), \theta_D(1)$. A dataset with 250 points was used to evaluate the function values in a grid with resolution 0.05 units.

dataset sizes and not generalize well enough. From now on, we will use the following nomenclature and color code to refer to the different models:

- LS-Ex (red): This is the benchmark model representing the classical open-loop approach. It uses LS to estimate demand and an exogenous reserve requirement.
- LS-Opt (blue): This is a partially optimized model, where least squares are used to estimate demand and only reserves requirements are optimized.
- Opt-Ex (yellow): This is also a partially optimized model, where demand is optimized whereas reserves requirements are still exogenously defined. This model is not particularly meaningful in practice. We show it in some studies, mostly for completeness.
- Opt-Opt (green): This is the fully optimized model, where both demand forecast and reserve requirements are jointly optimized.

For didactic purposes, in all cases tested in this section, up and down reserve requirements were defined as ± 1.96 standard deviations, respectively, of the estimated residuals from the LS demand forecast. Note, however, that other exogenous *ad hoc* rule could be used (Ela et al. 2011).

We empirically compare and analyze the convergence of the four demand and reserve requirement forecast models mentioned above. We varied the dataset size used in the estimation process from

50 to 1000 observations. For each dataset size, we performed 100 trial estimations, with different datasets generated from the same process, to study the convergence. To evaluate the out-of-sample performance of each one of the 100 estimates for each dataset size, we compute the objective function, G_a in (1), for a single fixed dataset with 10,000 new observations (generated with the same underlying process but different from all other data used in the estimation processes). In the following plots, lines represent mean values among the 100 estimated costs with the in-sample or out-of-sample data, and shaded areas represent the respective 10% and 90% quantiles.

The average operation cost for each dataset size is presented in Figure 4. The vertical axis shows in-sample costs, while the horizontal axis shows the dataset size used for the estimation procedure. It is possible to see that the method that co-optimizes reserves requirements and demand forecasts finds lower cost than the others. This is expected because this method has more degrees of freedom (it is a relaxed version of the others) on the parameter estimation and this is the objective function being minimized. Also, as expected, the LS plus exogenous reserves requirement model finds higher costs than the others. For the same reason, it does not allow for improvements by the local optimization method as it can be seen as a constrained version of the others. The other two methods are always in between and *Opt-Ex* is always below *LS-Opt*, which shows that demand forecasting might have a larger effect than reserve allocation in this test system.

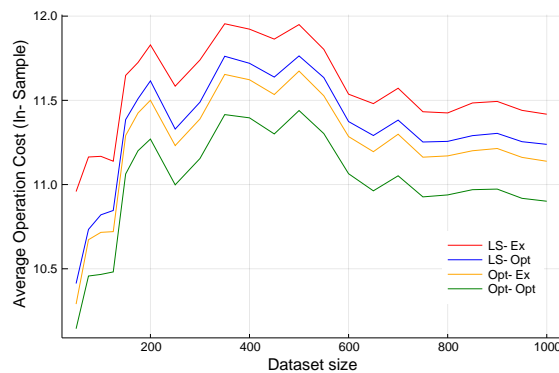
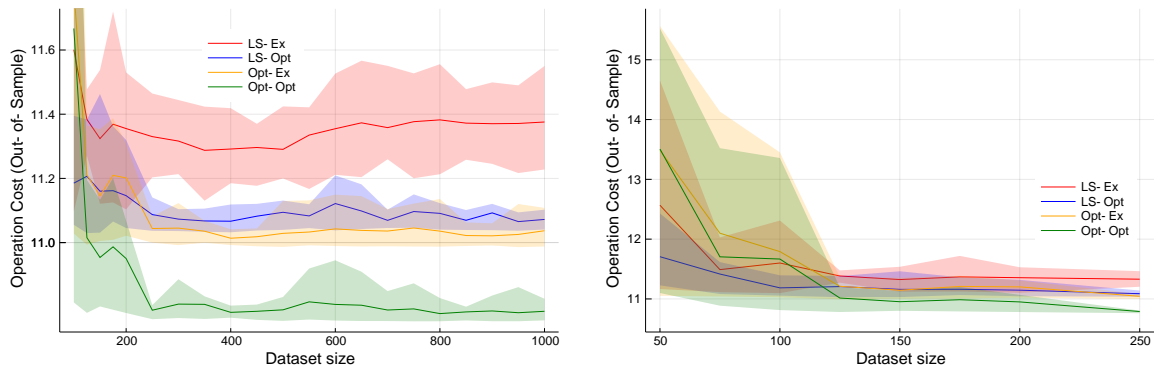


Figure 4 Average operation cost in training sample (in-sample) versus dataset size.

Figures 5 (a) and (b) depict the same costs but in the out-of-sample data. Hence, they measure how well the models generalize to data it has never seen before. We can see that the models allowing more parameters to be endogenously optimized perform much better than models with more exogenously defined forecast models. Thus, we see that the application-driven learning framework works successfully in out-of-sample data when estimated with datasets larger than 150. However, we note that these steady improvements require more data than the classic exogenous models, as shown in Figure 5 (b). Between 50 and 120 points, the model with more optimization flexibility, Opt-Opt, exhibits a more significant cost variance. This is due to excessive optimization in a small dataset that led to overfitting and poor generalization. Note that, in this work, we did not consider any regularization procedure to avoid this issue. However, our optimization based framework is suitable for well-known shrinkage operators (Tibshirani 2011) that can be readily added in the objective function (1).



(a) Starting from dataset size 200.

(b) Dataset size from 50 to 200.

Figure 5 Out-of-sample average operation cost versus (in-sample) dataset size. Lines represent the average of the 100 estimation trials. Shaded areas represent the 10% and 90% quantiles. All trials are evaluated on a single out-of-sample dataset with size 10,000 observations.

Figure 6 shows how the estimated parameters behave as functions of the estimation dataset size. In Figure 6 (a) and (b) we can see that the load model parameters are indeed converging to long-run values. It is also clear to see the bias in those parameters. The constant term is greatly

increased while the autoregressive coefficient is slightly reduced. Ultimately this leads to a larger forecast value, which can be interpreted as the application risk-adjustment due to the asymmetric imbalance penalization costs (load shed is much higher than the spillage cost). Thus, the Opt-Opt model will do the best possible to balance these costs, thereby prioritizing the load shed by increasing the forecast level. The fixed reserves model (Opt-Ex) is less biased because the fixed reserves constrain how much the load model can bias due to the risk of not having enough reserve to address lower demand realizations. Note that the red (LS-Ex) is on top of the purple (LS-Opt) since both use the same LS estimates for demand, which exhibits the lowest variance.

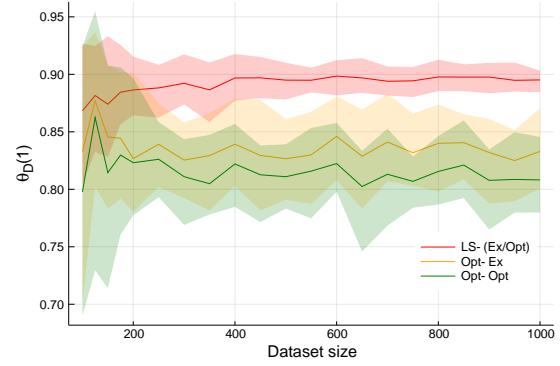
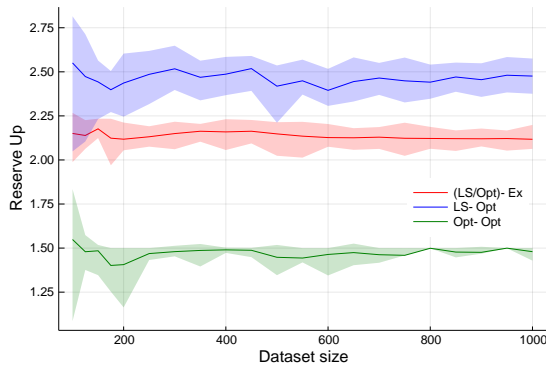
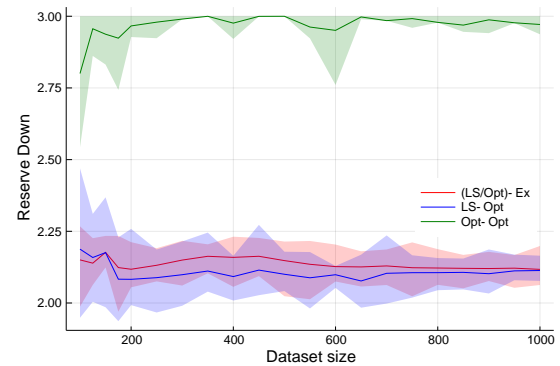
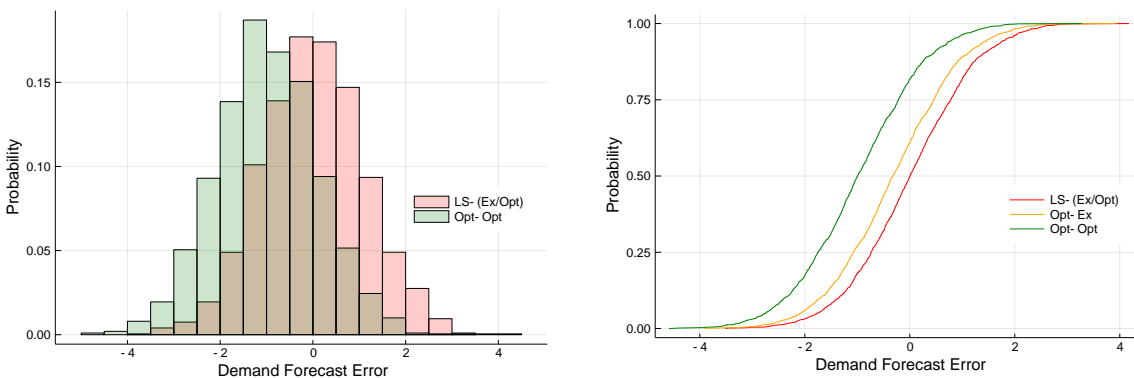
(a) $\theta_D(0)$, from (33)(b) $\theta_D(1)$, from (33)(c) Reserve up, $\theta_{R(up)}(0)$, from (34)(d) Reserve down, $\theta_{R(dn)}(0)$, from (35)

Figure 6 Estimated parameters versus dataset size. Lines represent the average of the 100 estimation trials. Shaded areas represent the 10% and 90% quantiles. (a) and (b) Load coefficients, the models LS-Ex and LS-Opt coincide, thereby are presented as LS-(Ex/Opt). (c) and (d) Reserve coefficients The models LS-Ex and Opt-Ex coincide, thereby are presented as (LS/Opt)-Ex.

In Figure 6 (c) and (d), we see that the Opt-Opt model greatly increases the downward reserve and decreases the upward reserve, both consistent with the change in the demand forecast parameters. Closed-loop estimation of only reserves led to increased up reserves that are the most expensive to violate, while downward reserves are mostly unaffected, this might be an artifact of the estimation model that uses the open-loop estimation as a starting point. The Opt-Opt model is limited in 3 because that is the maximum reserve that can be allocated (30% of the generators capacity).

To highlight the bias on load forecast we present, in Figure 7 (a), a histogram of deviations: $error := realization - forecast$. Negative values mean that the forecast value was above the realization. The LS estimation leads to an unbiased estimator, seen in the red histogram centered on zero. On the other hand, the forecast from the fully endogenous model is clearly biased, as it consistently forecasts higher values than the realizations. This fact is corroborated by the cumulative distribution functions displayed in Figure 7 (b).



(a) Two histograms are shown, the third color is their intersection (LS-Ex and LS-Opt coincide). (b) Accumulated Probability – out of the four models, three are shown here (LS-Ex and LS-Opt coincide).

Figure 7 Forecast error (observation – forecast) in a histogram, comparing fully optimized model with least squares estimation. Negative values mean forecast was larger than actual realization.

7.5. Dynamic reserves

This experiment aims to show that it is also possible to consider dynamic reserves within the proposed scheme, i.e., conditioned to external information being dynamically revealed to the system

operator. There are examples of works in the literature that considered the load to be heteroscedastic (Van der Meer et al. 2018). Hence, we will study here a simple formulation of demand time series with time-varying variance: We considered an exogenous variable E_t that follows an autoregressive process of order one (36) such that the variance of the real demand depends linearly on this new variable as shown in (37).

$$E_t = \phi(0) + \phi(1)E_{t-1} + \varepsilon_t, \quad \varepsilon_t \sim N(0, \sigma_E), \quad (36)$$

$$D_t = \theta_D(0) + \theta_D(1)D_{t-1} + \epsilon_t, \quad \epsilon_t \sim N(0, E_t), \quad (37)$$

We did not modify the demand forecast model (33), but we allowed for dynamic reserve sizing, that is, the reserve will vary with time. This time dependency will be considered through contextual information. As a driver for demand variance changes, E_t is a reasonable contextual information for estimating dynamic reserve margins. Thus, we consider the following models for the reserve requirements:

$$\hat{R}_t^{(up)} = \Psi_{R^{(up)}}(\theta_{R^{(up)}}, x_t) = \theta_{R^{(up)}}(0) + \theta_{R^{(up)}}(1)E_t, \quad (38)$$

$$\hat{R}_t^{(dn)} = \Psi_{R^{(dn)}}(\theta_{R^{(dn)}}, x_t) = \theta_{R^{(dn)}}(0) + \theta_{R^{(dn)}}(1)E_t. \quad (39)$$

The results of this experiment are depicted in Figure 8. We refer to the model from the previous sections as *static reserve* model, Figure 8 (a), and the model defined here as *dynamic reserve* model, Figure 8 (b). The system cost was clearly reduced by considering dynamic reserves for both Opt-Opt and LS-Opt models. In this case the Opt-Opt model gain over the LS-Opt is significantly reduced because the relevant part of the contextual information, E_t , concerns only with reserves margins. This happens because the optimal load forecast bias in the Opt-Opt model reduces to almost zero. This is a relevant insight that the proposed framework provides.

7.6. Reserves and demand forecast as a function of the load shed cost

This section aims to spotlight the dependency of the estimated parameters on the deficit cost, which is the largest violation penalty in this problem. We varied the deficit cost between 15 and 100 and estimated parameters with one single dataset with 1,000 observations.

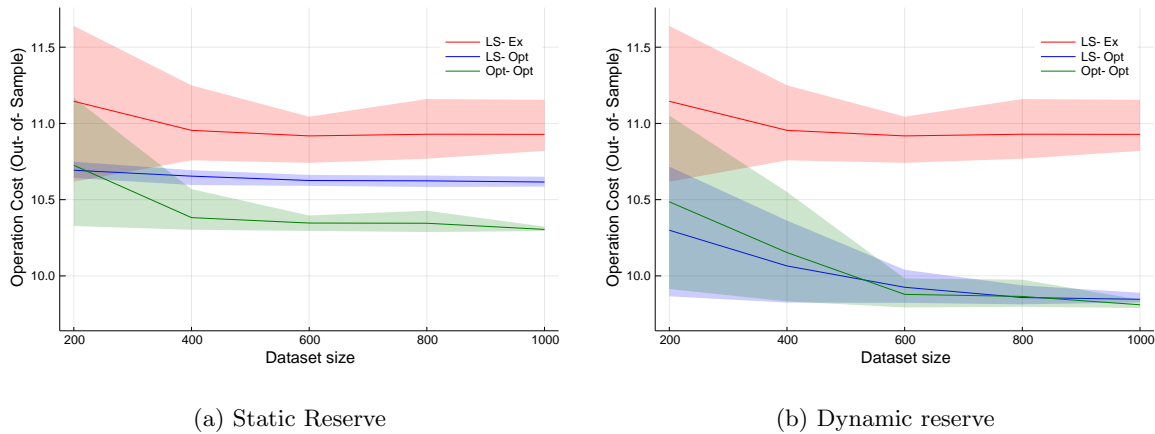


Figure 8 Variance driven by exogenous variable. Lines represent the average of the 100 estimation trials. Shaded areas represent the 10% and 90% quantiles.

Figure 9 depicts the up and down reserves and steady-state demand $(\theta_D(0)/(1 - \theta_D(1)))$. We added the solid line in red, *Demand LS*, to represent the steady-state demand and dashed red, *Reserve Ex*, to show the obtained reserve requirement from the residue of the LS estimation model. So, as these two values are exogenously calculated, they do not vary with the load shed cost. The solid green line, *Demand Opt-Opt*, shows an increasing bias as the load-shed cost grows, corroborating the expected behavior. The dashed green line also shows that the best response is to increase reserve levels as the load shed cost grows. The dashed blue lines are the reserve margins around the solid LS-based demand (red line) and they are also clearly affected by the load-shed cost.

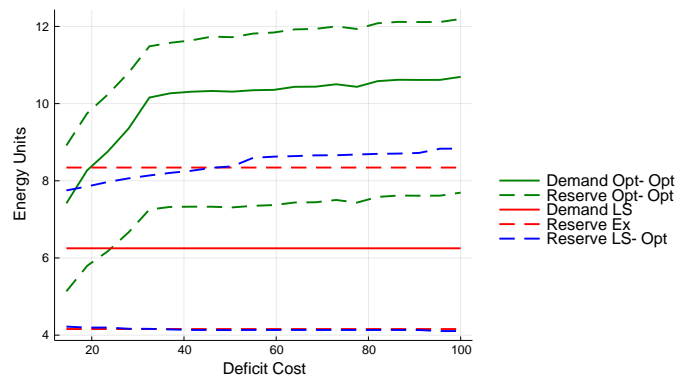


Figure 9 Long-run averages and reserve margins, in units of energy, as functions of deficit cost

7.7. Large scale optimization

In this final experiment, we apply the closed-loop estimation methodology to a larger power system network. As in the previous section, we focus our attention on the three models: LS-Ex, LS-Opt and Opt-Opt. Our primary goal in this case study is to demonstrate that the methodology can be applied to realistic power systems and that it is possible to obtain high-quality solutions that significantly improve the standard procedure. All results are depicted in Table 1

First, we can see that both closed-loop models consistently outperform the benchmark cost (LS-Ex) with almost 5% improvement in the out-of-sample evaluation for the 24-bus test system. There is not much value in estimating the demand endogenously in this system, although the endogenous reserve sizing improvement is evident. Second, in the 118-bus system, we see the same pattern again, a consistent improvement of the cost function by relying on the closed-loop models. This time we see a 3% improvement with both closed-loop models being similar to each other. Finally, in the 300-bus system, we can see consistent improvements once more. However, now we have a 5% improvement by endogenously sizing reserves and a 10% improvement by jointly estimating the closed-loop demand forecast and reserve size. Of course, the results come at the expense of increased computational cost, but the computation times are still reasonable, showing that the method can be used in real-world power systems.

System	Model	Test Cost(\$)		Train Cost (\$)		Train Time (s)	
		Mean	Std	Mean	Std	Mean	Std
24	LS-Ex	414.70	1.14	397.01	4.39	0.00	0.00
	LS-Opt	398.48	0.69	378.49	93.00	450.81	90.35
	Opt-Opt	398.20	1.04	376.35	14.04	643.89	11.16
118	LS-Ex	2956.01	11.33	3163.74	3.78	0.00	0.00
	LS-Opt	2829.86	4.20	3041.28	4.86	639.87	4.97
	Opt-Opt	2815.85	4.57	3029.93	13.20	911.43	12.37
300	LS-Ex	7697.25	40.78	7646.84	26.09	0.00	0.00
	LS-Opt	7329.44	36.62	7278.88	18.75	803.15	34.08
	Opt-Opt	6820.47	37.67	6787.65	294.53	2748.17	303.56

Table 1 Results for the 24, 118 and 300-bus systems

8. Conclusions

We presented a general application-driven framework to jointly estimate the parameters of a load and reserve requirements forecast model in a closed-loop fashion. A mathematical framework is proposed following the ideas of bilevel optimization. Asymptotic convergence is demonstrated and two solutions techniques are presented. The proposed method is contrasted with the classical sequential open-loop procedure where the forecast models are estimated based on least squares and used in the decision-making process. Regarding our application case, the proposed framework finds support in current industry practices, where *ad hoc* procedures are implemented to bias load forecasts to empirically reduce risks. The application of our model provides not only a theoretically-grounded understanding of such procedures, but also a flexible computational tool for testing current practices and jointly determining the optimal bias and reserve requirements.

The reported numerical experience allows highlighting the following main empirical results and insights: 1) There exists an optimal bias in the load forecast maximizing the performance of a system or market operator in the long-run. Moreover, the optimal bias in the load forecast is not disconnected from the optimal reserve requirements (reserve sizing problem); 2) Reserve sizing is intrinsically dependent on the load-shed cost and system's characteristics and can be optimally determined by our framework even in the case where traditional methods exogenously estimate the demand forecast; 3) Our model can endogenously define the optimal reserve sizing across the network by defining zonal reserve requirements that will best perform given the system operator's description of the network; 4) We show for realistic test systems, e.g., IEEE 300-bus system, that a model only estimating the reserve requirements is capable of improving 4.8% the long-run operation cost and 11.4% when co-optimizing load forecasts and reserve requirement; 5) We show that the proposed heuristic solution method can provide high-quality solutions in reasonable computational time. This is mostly due to the selected approach, which i) initializes the search method with the traditional least-square estimates, thereby only moving to another point if an improvement in performance is found, and ii) allows the estimation problem to be decomposed per observation and

the second-level problem to be solved till global optimality in polynomial time. Additionally, it also leverages mature linear-programming-based warm-start technologies and algorithms to scale up the performance in larger instances. This pattern is consistently observed in all test systems, corroborating the proposed framework’s effectiveness in finding improved estimates for both load and reserve requirements.

The proposed framework is fairly general, but we focused on right hand side uncertainty and linear models as this was the relevant setting for the reserve requirement forecasting problem. Possible extensions of this work could aim at generalizing this setting. Indeed, the exact method would work for objective-function uncertainty and for non-linear models with strong duality like many conic programs. The heuristic method is even more flexible, it could accommodate uncertainty anywhere in the models and it could be used in many non-linear (even integer) problems. Other aspects of estimation procedures to be explored include regularization with shrinkage operators (Tibshirani 2011), or the addition of LS estimates in the objective (Kao et al. 2009) with a penalizing coefficient to provide a balance between classical and application-driven forecasts. Moreover, it would be interesting to conduct experiments to verify the empirical performance of various statistical models (ψ) such as vector auto-regressive models. Proving convergence conditions for many of the aforementioned changes in the model would provide nice contributions to the literature.

References

- Aravena I, Papavasiliou A (2020) Asynchronous lagrangian scenario decomposition. *Mathematical Programming Computation* 1–50.
- Babaeinejadsarookolae S, Birchfield A, Christie RD, Coffrin C, DeMarco C, Diao R, Ferris M, Fliscounakis S, Greene S, Huang R, et al. (2019) The power grid library for benchmarking ac optimal power flow algorithms. *arXiv preprint arXiv:1908.02788* .
- Bard JF (2013) *Practical bilevel optimization: algorithms and applications*, volume 30 (Springer Science & Business Media).
- Bengio Y (1997) Using a financial training criterion rather than a prediction criterion. *International Journal of Neural Systems* 8(04):433–443.

- Bertsimas D, Kallus N (2019) From predictive to prescriptive analytics. *Management Science* .
- Böhm V (1975) On the continuity of the optimal policy set for linear programs. *SIAM Journal on Applied Mathematics* 28(2):303–306.
- Borrelli F, Bemporad A, Morari M (2003) Geometric algorithm for multiparametric linear programming. *Journal of optimization theory and applications* 118(3):515–540.
- Bucksteeg M, Niesen L, Weber C (2016) Impacts of dynamic probabilistic reserve sizing techniques on reserve requirements and system costs. *IEEE Transactions on Sustainable Energy* 7(4):1408–1420.
- CAISO (2020) 2019 Annual Report on Market Issues and Performance. Department of Market Monitoring, California Independent System Operator. URL <http://www.caiso.com/Documents/2019AnnualReportonMarketIssuesandPerformance.pdf>.
- Chen Y, Gribik P, Gardner J (2013) Incorporating post zonal reserve deployment transmission constraints into energy and ancillary service co-optimization. *IEEE Transactions on Power Systems* 29(2):537–549.
- Conn AR, Scheinberg K, Vicente LN (2009) *Introduction to derivative-free optimization* (SIAM).
- De Vos K, Stevens N, Devolder O, Papavasiliou A, Hebb B, Matthys-Donnadieu J (2019) Dynamic dimensioning approach for operating reserves: Proof of concept in belgium. *Energy policy* 124:272–285.
- Dempe S (2018) *Bilevel optimization: theory, algorithms and applications* (TU Bergakademie Freiberg, Fakultät für Mathematik und Informatik).
- Dias Garcia J, Bodin G, and contributors (2021) joaquimg/bileveljump.jl: v0.4.1. URL <http://dx.doi.org/10.5281/zenodo.4556393>.
- Donti P, Amos B, Kolter JZ (2017) Task-based end-to-end model learning in stochastic optimization. *Advances in Neural Information Processing Systems*, 5484–5494.
- Dunning I, Huchette J, Lubin M (2017) Jump: A modeling language for mathematical optimization. *SIAM Review* 59(2):295–320.
- Ela E, Milligan M, Kirby B (2011) Operating reserves and variable generation. Technical Report NREL/TP-5500-51978, National Renewable Energy Lab. (NREL), Golden, CO (United States).
- Elmachtoub AN, Grigas P (2017) Smart” predict, then optimize”. *arXiv preprint arXiv:1710.08005* .

- Fortuny-Amat J, McCarl B (1981) A representation and economic interpretation of a two-level programming problem. *Journal of the Operational Research Society* 32(9):783–792.
- Franceschi L, Frasconi P, Salzo S, Grazzi R, Pontil M (2018) Bilevel programming for hyperparameter optimization and meta-learning. *International Conference on Machine Learning*, 1568–1577 (PMLR).
- Gade D, Hackebeil G, Ryan SM, Watson JP, Wets RJB, Woodruff DL (2016) Obtaining lower bounds from the progressive hedging algorithm for stochastic mixed-integer programs. *Mathematical Programming* 157(1):47–67.
- Gal T (2010) *Postoptimal Analyses, Parametric Programming, and Related Topics: degeneracy, multicriteria decision making, redundancy* (Walter de Gruyter).
- Garcia R, Gençay R (2000) Pricing and hedging derivative securities with neural networks and a homogeneity hint. *Journal of Econometrics* 94(1-2):93–115.
- Henningsen A, Toomet O (2011) maxlik: A package for maximum likelihood estimation in r. *Computational Statistics* 26(3):443–458.
- Holttinen H, Milligan M, Ela E, Menemenlis N, Dobschinski J, Rawn B, Bessa RJ, Flynn D, Gomez-Lazaro E, Detlefsen NK (2012) Methodologies to determine operating reserves due to increased wind power. *IEEE Transactions on Sustainable Energy* 3(4):713–723.
- Hong T, Fan S (2016) Probabilistic electric load forecasting: A tutorial review. *International Journal of Forecasting* 32(3):914–938.
- Kao Yh, Roy BV, Yan X (2009) Directed regression. *Advances in Neural Information Processing Systems*, 889–897.
- Kazempour J, Pinson P, Hobbs BF (2018) A stochastic market design with revenue adequacy and cost recovery by scenario: Benefits and costs. *IEEE Transactions on Power Systems* 33(4):3531–3545.
- Kirschen DS, Strbac G (2018) *Fundamentals of power system economics* (John Wiley & Sons).
- Knueven B, Ostrowski J, Watson JP (2020) On mixed-integer programming formulations for the unit commitment problem. *INFORMS Journal on Computing* 32(4):857–876.
- Li H, Bose A, Venkatasubramanian VM (2015) Wide-area voltage monitoring and optimization. *IEEE Transactions on Smart Grid* 7(2):785–793.

- Megiddo N, Chandrasekaran R (1989) On the ε -perturbation method for avoiding degeneracy. *Operations Research Letters* 8(6):305–308.
- Mogensen PK, Riseth AN (2018) Optim: A mathematical optimization package for julia. *Journal of Open Source Software* 3(24).
- Muñoz MA, Pineda S, Morales JM (2020) A bilevel framework for decision-making under uncertainty with contextual information. *arXiv preprint arXiv:2008.01500* .
- Nocedal J, Wright S (2006) *Numerical optimization* (Springer Science & Business Media).
- Orwig KD, Ahlstrom ML, Banunarayanan V, Sharp J, Wilczak JM, Freedman J, Haupt SE, Cline J, Bartholomy O, Hamann HF, et al. (2014) Recent trends in variable generation forecasting and its value to the power system. *IEEE Transactions on Sustainable Energy* 6(3):924–933.
- Papavasiliou A, Oren SS (2013) Multiarea stochastic unit commitment for high wind penetration in a transmission constrained network. *Operations Research* 61(3):578–592.
- Papavasiliou A, Oren SS, Rountree B (2014) Applying high performance computing to transmission-constrained stochastic unit commitment for renewable energy integration. *IEEE Transactions on Power Systems* 30(3):1109–1120.
- Pereira MV, Granville S, Fampa MH, Dix R, Barroso LA (2005) Strategic bidding under uncertainty: a binary expansion approach. *IEEE Transactions on Power Systems* 20(1):180–188.
- PJM (2018) PJM Manual 11 : Energy and Ancillary Services Market Operations (97):200, URL <https://pjm.com/-/media/documents/manuals/archive/m11/m11v97-energy-and-ancillary-services-market-operations-07-26-2018.ashx>.
- Rockafellar RT, Uryasev S, Zabarankin M (2008) Risk tuning with generalized linear regression. *Mathematics of Operations Research* 33(3):712–729.
- Ryzhov IO, Powell WB (2012) Information collection for linear programs with uncertain objective coefficients. *SIAM Journal on Optimization* 22(4):1344–1368.
- Sen S, Deng Y (2018) Learning enabled optimization: Towards a fusion of statistical learning and stochastic programming. *Optimization Online* .

- Shapiro A, Dentcheva D, Ruszczyński A (2014) *Lectures on stochastic programming : modeling and theory* (SIAM), 2nd edition.
- Siddiqui S, Gabriel SA (2013) An sos1-based approach for solving mpecs with a natural gas market application. *Networks and Spatial Economics* 13(2):205–227.
- Strbac G, Shakoor A, Black M, Pudjianto D, Bopp T (2007) Impact of wind generation on the operation and development of the uk electricity systems. *Electric Power Systems Research* 77(9):1214–1227.
- Sweeney C, Bessa RJ, Browell J, Pinson P (2020) The future of forecasting for renewable energy. *Wiley Interdisciplinary Reviews: Energy and Environment* 9(2):e365.
- The European Commission (2017) Commission regulation (eu) 2017/1485 - establishing a guideline on electricity transmission system operation.
<https://eur-lex.europa.eu/legal-content/EN/TXT/HTML/?uri=CELEX:32017R1485&from=EN>.
- Tibshirani R (2011) Regression shrinkage and selection via the lasso: a retrospective. *Journal of the Royal Statistical Society: Series B (Statistical Methodology)* 73(3):273–282.
- Van der Meer DW, Widén J, Munkhammar J (2018) Review on probabilistic forecasting of photovoltaic power production and electricity consumption. *Renewable and Sustainable Energy Reviews* 81:1484–1512.
- Varian H (1975) A bayesian approach to real estate assessment. Fienberg SE, Zellner A, eds., *Studies in Bayesian Econometrics and Statistics in Honor of Leonard J. Savage* (Amsterdam: North-Holland).
- Wang B, Hobbs BF (2014) A flexible ramping product: Can it help real-time dispatch markets approach the stochastic dispatch ideal? *Electric Power Systems Research* 109:128–140.
- Wang B, Hobbs BF (2015) Real-time markets for flexiramp: A stochastic unit commitment-based analysis. *IEEE Transactions on Power Systems* 31(2):846–860.
- Zellner A (1986a) Bayesian estimation and prediction using asymmetric loss functions. *Journal of the American Statistical Association* 81(394):446–451.
- Zellner A (1986b) Biased predictors, rationality and the evaluation of forecasts. *Economics Letters* 21(1):45–48.
- Zheng QP, Wang J, Liu AL (2014) Stochastic optimization for unit commitment—a review. *IEEE Transactions on Power Systems* 30(4):1913–1924.